ChemPubSoc Europe

DOI: 10.1002/chem.201603156

CHEMISTRY
A European Journal
Full Paper

Surface Chemistry | *Hot Paper* |

Photocontrolled On-Surface Pseudorotaxane Formation with Well-Ordered Macrocycle Multilayers

Felix B. Schwarz,[a] Thomas Heinrich,[a, b] J. Ole Kaufmann,[a] Andreas Lippitz,[b]
Rakesh Puttreddy,[c] Kari Rissanen,[c] Wolfgang E. S. Unger,*[b] and Christoph A. Schalley*[a]

Abstract: The photoinduced pseudorotaxane formation between a photoresponsive axle and a tetralactam macrocycle was investigated in solution and on glass surfaces with immobilized multilayers of macrocycles. In the course of this reaction, a novel photoswitchable binding station with azobenzene as the photoswitchable unit and diketopiperazine as the binding station was synthesized and studied by NMR and UV/Vis spectroscopy. Glass surfaces have been functionalized with pyridine-terminated SAMs and subsequently with multilayers of macrocycles through layer-by-layer self assembly. A preferred orientation of the macrocycles could be confirmed by NEXAFS spectroscopy. The photocontrolled deposition of the axle into the surface-bound macrocycle-multilayers was monitored by UV/Vis spectroscopy and led to an increase of the molecular order, as indicated by more substantial linear dichroism effects in angle-resolved NEXAFS spectra.

Introduction

Stimuli-responsive chemical systems capable of performing molecular motion are of great interest for the development of functional materials and molecular machines.[1] Immobilizing such molecules on surfaces allows the concerted action of molecular switches and shuttles.[2] In particular, surfaces functionalized with photoresponsive units have been of great interest in recent research.[3] Mostly, gold and silicon substrates have been used as they can be easily functionalized with well-studied monolayers and due to the technological importance of these substrates.[4] Photochromic molecules like azobenzenes, spiropyranes, or dithienylethenes bound to surfaces have, for example, been used to control the surface wettability,[5] to change their electrical properties,[6] or to control the adsorption of molecules on surfaces.[7] Furthermore, photoresponsive units were utilized to actuate and control the molecular motion in molecular rotary motors[8] and linear molecular muscles.[9]

Recently, we reported the deposition of ordered multilayers of Hunter/Vögtle-type tetralactam macrocycles[10] (TLM) and TLM-based rotaxanes[11] on different substrates through layer-by-layer self-assembly[12] using metal-ion/pyridine/terpyridine coordination chemistry.[13] This included the implementation of chemically switchable rotaxanes that change the macrocycle position in a cooperative manner when adding or removing chloride ions.[14] Although these systems work nicely, addressing responsive surfaces by inducing a chemical stimulus has some limitations. It unavoidably brings impurities into the system and, therefore, hampers an unambiguous analysis of structural changes on the surface. Another problem could be to address the lower layers in densely packed systems, which bulky molecules cannot reach easily by diffusion. In order to overcome these limitations, we aim to implement photoswitchable molecules in these previously realized macrocycle multilayer surfaces.

In this study, we start with a photoswitchable pseudorotaxane as the precursor for further studies with rotaxanes. Azobenzene, one of the most studied photochromic molecules, was chosen as the photoswitchable unit due to its fast and clean photoisomerization associated with different geometric and physicochemical properties of the two switching states.[15] The outstanding optomechanical properties make azobenzene a key compound in switchable molecular and supramolecular functional systems, which is reflected in various reported examples in solution,[16] on nanoparticles,[17] and on surfaces.[18] However, there are only a few reports on surface-[19] or nanoparticle-bound[20] azobenzene-based (pseudo-)rotaxanes.

To utilize the *cis–trans* photoisomerization of azobenzene for controlling the threading and dethreading of a pseudorotaxane with a Hunter/Vögtle-type TLM, the photoswitch was attached to a rigid xanthene backbone resulting in a fixed position relative to the diketopiperazine binding station to influence its binding strength by steric hindrance. While the azobenzene

---

[a] *F. B. Schwarz, T. Heinrich, J. O. Kaufmann, Prof. C. A. Schalley*
Institut für Chemie und Biochemie, Freie Universität Berlin
Takustrasse 3, 14195 Berlin (Germany)
E-mail: c.schalley@fu-berlin.de

[b] *T. Heinrich, A. Lippitz, Dr. W. E. S. Unger*
BAM-Federal Institute for Materials Research and Testing
Unter den Eichen 44-46, 12203 Berlin (Germany)
E-mail: wolfgang.unger@bam.de

[c] *Dr. R. Puttreddy, Acad. Prof. K. Rissanen*
University of Jyvaskyla, Department of Chemistry
Nanoscience Center, P.O. Box. 35, 40014 Jyvaskyla (Finland)

Supporting information for this article can be found under http://dx.doi.org/10.1002/chem.201603156.

blocks the binding station in its *trans* configuration, the binding site becomes available upon switching to the *cis* isomer. In solution studies by Jeong et al.,[21] a similar photoswitchable diamide station exhibited binding to nitro-substituted macrocycles. For our purposes, such a substitution on the macrocycles isophthaloyl diamide units is not suitable as it would block the functionalization necessary for surface binding. To design a suitable molecule for binding in our TLM multilayer surfaces, we have introduced diketopiperazine as the binding station, which exhibits a higher binding affinity towards TLM.[22]

Results and Discussion

The photoswitchable binding site **8** was synthesized starting from commercially available xanthene **1** by following literature known procedures[21b,23] to give the azobenzene-substituted xantheneamine **4**. The synthesis was optimized to achieve higher product yields (for details see the Supporting Information). The diketopiperazine binding station was attached to amine **4** in four steps[24] starting with the reaction of **4** with bromoacetic acid ethyl ester to give secondary amine **5**. Compound **5** was then acetylated with chloroacetyl chloride and subsequently converted to iodide **6** in a Finkelstein reaction. Treatment of **6** with methanolic ammonia induced ring closure and afforded the diketopiperazine **7**. Methylation of **7** yielded the final product **8** with an overall yield of 14% over 10 steps (Scheme 1). Tetralactam macrocycles were synthesized according to literature known procedures.[25]

Single crystals of *trans*-**7** suitable for X-ray analysis (Supporting Information) were obtained by the slow evaporation of a solution of *trans*-**7** in methanol. Figure 1 a shows the section of the asymmetric unit of *trans*-**7**, crystallized in the triclinic space group $P\bar{1}$ with selected atom labeling. The asymmetric unit contains two *trans*-**7** and two water molecules. The restricted rotation of the diketopiperazine, due to steric hindrance with the xanthene-substituted azobenzene, favors the keto-groups as binding stations in **8@9**. The azobenzene is in its *trans* configuration with the phenyl ring, and is nearly coplanar to the xanthene-backbone with a root mean square deviation (RMSD) of 0.140 Å. The angle between the mean planes

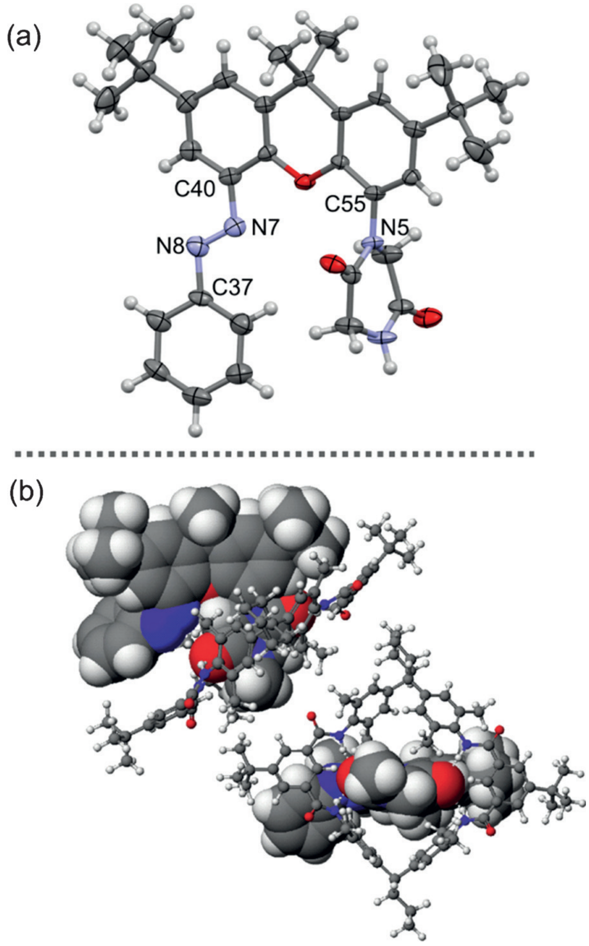

Figure 1. a) Crystal structure of **7** (thermal ellipsoids are shown at the 50% probability level) and b) MM2 force-field model of the pseudorotaxane **8@9** with axle **8** displayed in space-filling mode and macrocycle **9** in a ball-and-stick model (top left: side view, bottom right: top view). See the Supporting Information for a crystal structure of **9**.

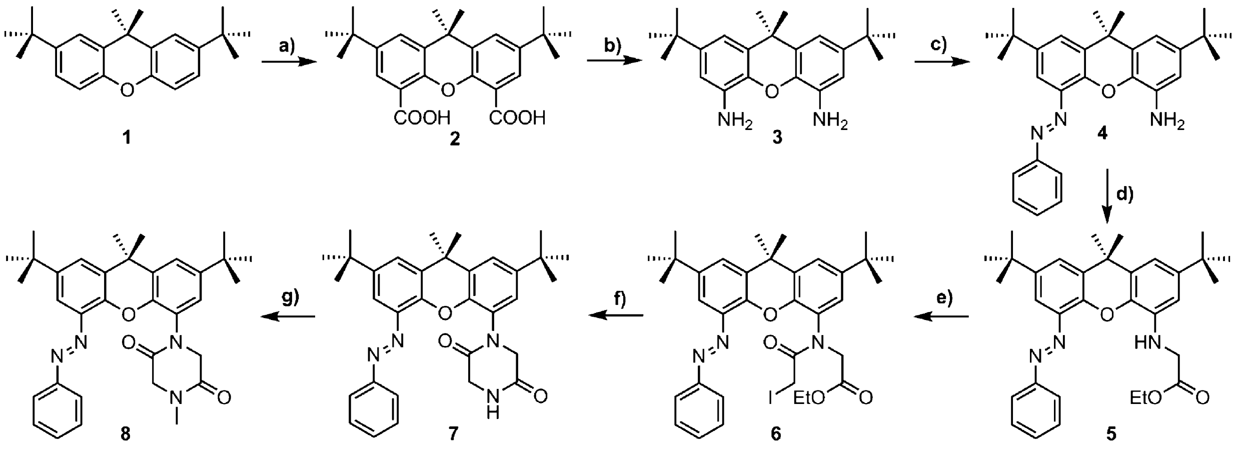

Scheme 1. Synthesis of photoswitchable binding station **8**: a) 1. Br_2, $CHCl_3$, rt, 24 h, quant., 2. *n*BuLi, CO_2, THF, −78 °C, 2 h, 62%; b) 1. DPPA, TEA, BnOH, toluene, 80 °C, 22 h, 79%, 2. KOH, EtOH, 90 °C, 16 h, 98%; c) Nitrosobenzene, HOAc, $CHCl_3$, rt, 17 h, 54%; d) Ethyl bromoacetate, $NaHCO_3$, DMF, 90 °C, 20 h, 76%; e) 1. Chloroacetyl chloride, TEA, CH_2Cl_2, 0 °C→rt, 12 h, 83%, 2. NaI, acetone, rt, 16 h, 99%. f) NH_3 in MeOH, MeOH, rt, 12 h, 89%. g) KO*t*Bu, MeI, THF, 0 °C→rt, 98%. DPPA = diphenylphosphoryl azide; TEA = **t**riethylamine.

of these rings is 86.7°. The diketopiperazine rings in two crystallographically independent molecules constitutes a RMSD of 0.132 and 0.58, and are perpendicular to the xanthene backbone. All the bond parameters in the xanthene backbone of **7** and C55–N5 (1.440(4) Å) are close to the reported values,[26] while C40–N7 (1.423(4) Å), N7–N8 (1.261(4) Å), and N8–C37 (1.429(4) Å) are similar to *trans*-azobenzene.[27]

MM2 force-field modeling shows *cis*-**8** to nicely fit into the cavity of the TLM (Figure 1 b). The modeled structure is in good agreement with the crystal structure of **7** in which the xanthene unit is almost planar, while the diketopiperazine unit is turned out of plane.

The photoisomerization of **8** and subsequent pseudorotaxane formation (Figure 2 a) was studied first in solution by UV/Vis and NMR spectroscopy. The di-*tert*-butyl-substituted TLM **9** (for an X-ray structure, see the Supporting Information) was used for solution studies due to its good solubility. Photoisomerization of **8** from *trans* to *cis* was carried out by irradiating a solution of *trans*-**8** in CH_2Cl_2 with an LED lamp at a wavelength of $\lambda_1 = 365$ nm. The back isomerization to the *trans* configuration was performed by either irradiation with an LED lamp at $\lambda_2 = 470$ nm or by equilibration in the dark at room temperature for 24 h.

The UV/Vis spectrum of *trans*-**8** in CH_2Cl_2 (Figure 2 b) shows the characteristic absorption band for the $\pi \rightarrow \pi^*$ transition of the azobenzene at 323 nm,[28] which decreases upon irradiation with $\lambda_1 = 365$ nm, indicating the formation of *cis*-**8**. The photostationary state with a *cis*- to *trans*-**8** ratio of 2:1 was reached after approximately 10 min. After irradiation with $\lambda_2 = 470$ nm for 10 min or equilibration in the dark over 24 h, the UV/Vis spectrum was hardly different from the initial one. Reversibility was tested by alternating irradiation over five cycles (Figure 2 c). UV/Vis analysis of **8** was also carried out with a 1:1 mixture of **8** and **9**, in which, as expected, no shifts of absorption maxima could be observed since the binding mode does not significantly influence the chromophor's electronic properties.

Besides investigating the switching process and its reversibility by UV/Vis spectroscopy, NMR spectroscopy was applied to gain structural information and evidence for switchable pseudorotaxane formation. The NMR spectrum of TLM **9** (Figure 2 d, I) shows the signals for the inner isophthalic acid protons **a** at 7.98 ppm and the amide protons **b** at 7.29 ppm. Upon addition of one equivalent *trans*-**8** (Figure 2 d, II), the amide protons undergo only a very small shift of $\Delta\delta = 0.04$ ppm. After 10 min irradiation at $\lambda_1 = 365$ nm (Figure 2 d, III), a second set of signals for *cis*-**8** appears with a ratio of *cis*- to *trans*-**8** of approximately 2:1. Due to a fast exchange of axle **8** in the cavity of macrocycle **9**, averaged signals are observed. The macrocycle protons **a** and **b** are now significantly shifted downfield by $\Delta\delta =$

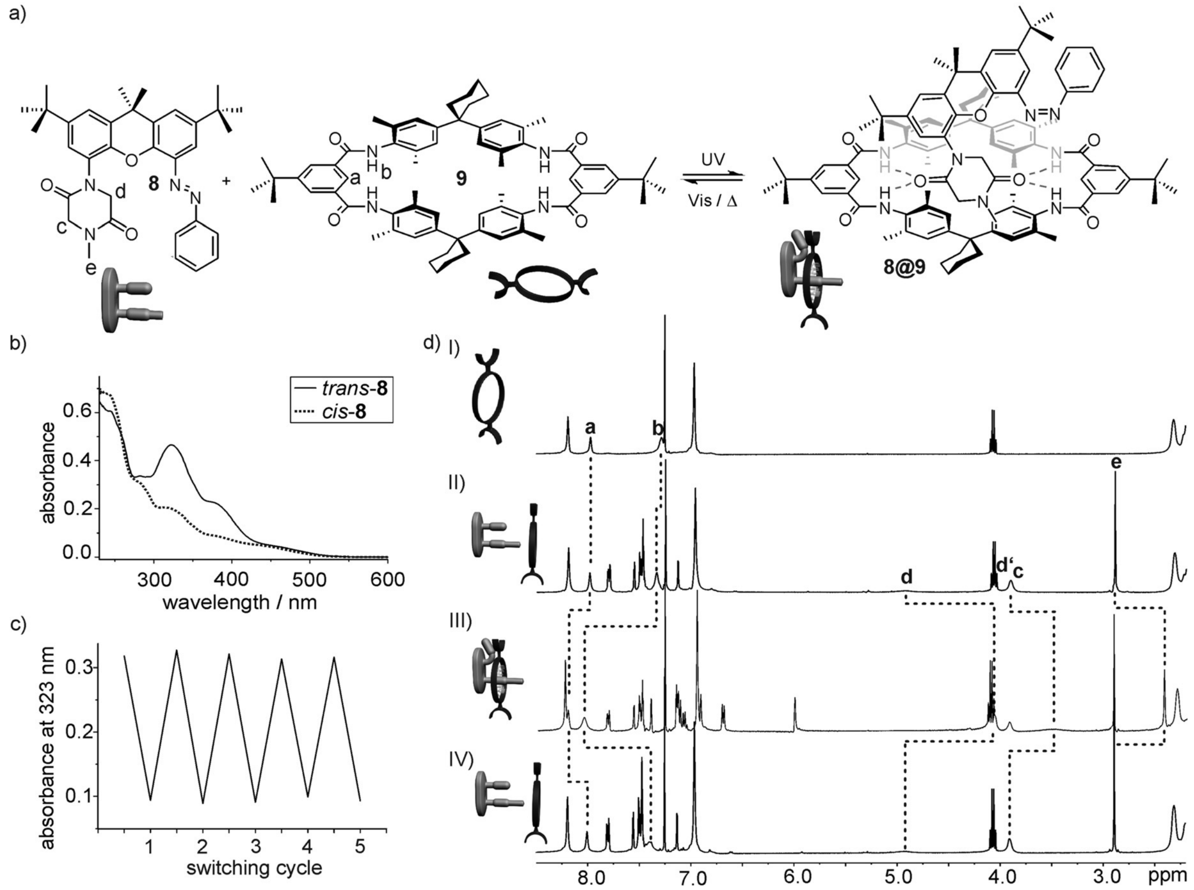

Figure 2. a) Photoswitchable pseudorotaxane formation. b) UV/Vis spectra of *cis*- and *trans*-**8** in CH_2Cl_2. c) Reversibility of photoswitching in CH_2Cl_2 tested by alternating irradiation at $\lambda_1 = 365$ nm and $\lambda_2 = 470$ nm for 10 min in each step. d) NMR analysis (400 MHz, 298 K, $CDCl_3$) of pseudorotaxane switching. I: TLM **9**. II: **9** + *trans*-**8**, 1:1. III: **9** + **8** after 10 min irradiation at $\lambda_1 = 365$ nm. IV: **9** + **8** after 24 h in the dark at rt.

0.21 ppm and $\Delta\delta = 0.86$ ppm due to hydrogen bonding to *cis*-**8**. The axle protons **c**, **d**, and **e** are shifted upfield by $\Delta\delta = 0.44$, 0.88, and 0.49 ppm due to the shielding effect of TLM **9**, clearly evidencing pseudorotaxane formation. After leaving the sample for 24 h in the dark, the spectrum was virtually indistinguishable from the initial one (Figure 2d, IV). When the back isomerization was carried out photochemically by irradiation at $\lambda_2 = 470$ nm, the photostationary state with a *cis*- to *trans*-**8** ratio of 1:9 was reached after approximately 10 min, as determined by NMR (for the spectrum see the Supporting Information).

Binding constants of *trans*- and *cis*-**8** to TLM **9** have been determined by NMR titrations. For *trans*-**8**, a very small binding constant of $<15\,\text{M}^{-1}$ was obtained (Supporting Information), while *cis*-**8** has a binding constant of $1{,}650 \pm 165\,\text{M}^{-1}$ (Figure 3).

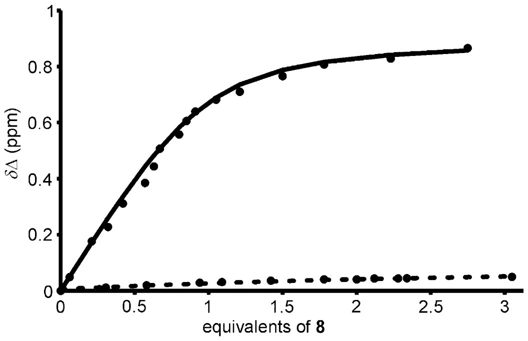

Figure 3. NMR titration of TLM **9** with *trans*-**8** (-----) and *cis*-**8** (——) in $CDCl_3$ at room temperature.

After studying pseudorotaxane formation and its switchability in solution, the concept was transferred to surfaces. Multilayers of tetralactam macrocycles have been prepared by metal-coordination-based layer-by-layer self-assembly on glass substrates according to previously established procedures.[29]

As the template layer, a self-assembled monolayer of **PDS** (Figure 4a) was deposited on cleaned glass surfaces. The surfaces were then treated with a 1 mM solution of $Pd(CH_3CN)_4(BF_4)_2$ in CH_2Cl_2 to coordinate the pyridyl endgroups of the SAM with Pd^{II} ions, enabling the attachment of the next organic layer. By alternating deposition of di-terpyridine-TLM **10** and $Fe(BF_4)_2{\cdot}6H_2O$, a controlled growth of macrocycle layers was achieved, monitored by UV/Vis spectra recorded after each deposition step (Figure 4b).

To show that *cis*-**8** binds to the cavity of the macrocycles on the surface while *trans*-**8** does not, surfaces with one, three, and five layers of TLM **10** have been prepared. A surface with only the SAM was used as the control. The surfaces were immersed in a 1 mM solution of *trans*-**8** (large excess) in CH_2Cl_2 for 24 h, followed by immersing the surface in CH_2Cl_2 for 10 min to remove any unspecifically bound molecules. For all four surfaces, no increase of the π–π* band in the UV/Vis spectra before and after immersion to the solution of *trans*-**8** was observed, clearly showing that no additional chromophores are deposited on the surface and therefore that *trans*-**8** does not bind to the macrocycle multilayers (Figure 4c).

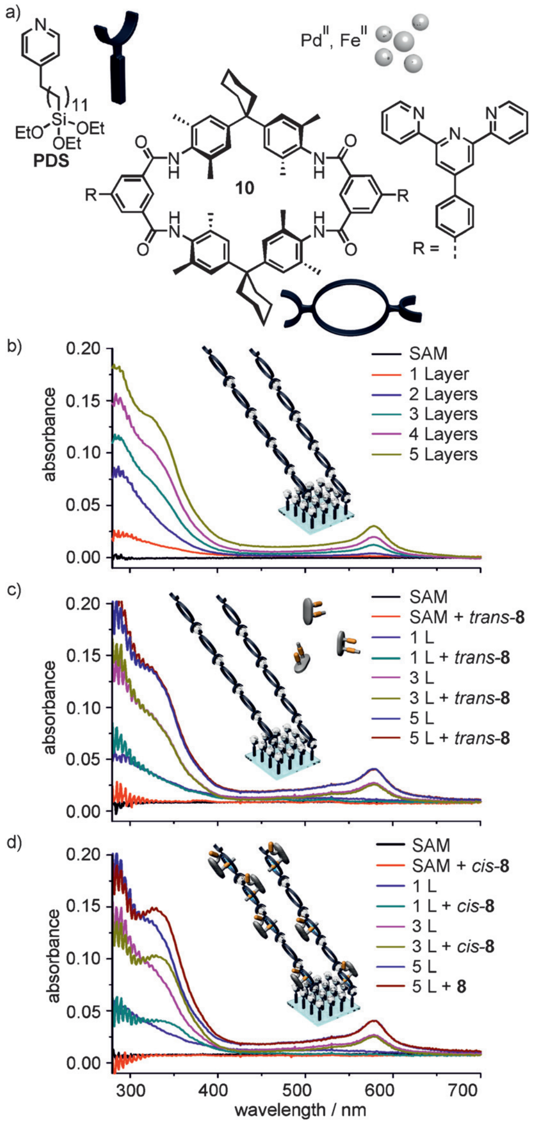

Figure 4. a) Diterpyridine-TLM **10**, **PDS**-SAM, metal ions used for the self-assembly of macrocycle multilayers. b) Surface UV/Vis spectra showing multilayer deposition. c) UV/Vis spectra of surfaces before and after immersion in *trans*-**8** solution. d) UV/Vis spectra of surfaces before and after immersion in *cis*-**8** solution. The increase of absorption in 4d is in line with the solution UV/Vis spectra of *cis*-**8** in Figure 2b.

The experiment was then repeated with the same surfaces immersed into the same solution, but now under continuous irradiation with UV light of a wavelength of $\lambda_1 = 365$ nm to form *cis*-**8**.

To avoid light-induced damage on the surfaces, the irradiation was carried out in a way that no light reached the surfaces directly, but only the solution was irradiated. After washing the surfaces for 10 min with CH_2Cl_2, UV/Vis spectra were recorded. The spectrum of the surface with only the **PDS**-SAM showed no change before and after deposition of **8**. The spectra of the surfaces with one, three, and five layers of TLM **10** showed a substantial increase of the absorption around 350 nm, indicating the deposition of *cis*-**8** (Figure 4d).

Interestingly, the increase of absorption after the deposition of **8** on the surfaces does not linearly increase with a higher number of macrocycle layers. While the absorption increases for three layers relative to one layer, it does not increase any further for five layers (Supporting Information). This indicates that the multilayers are rather densely packed and that not all macrocycles are accessible for the binding of *cis*-**8**. In a previous study, we used a squaraine as the guest molecule that was bound to macrocycle multilayers and a linear increase of bound molecules with an increasing number of layers was observed.[30] This can be explained by the differences between the molecular structure of the guests. While the squaraine molecule used in the former study is relatively small, has a linear form without stopper-units and can therefore easily slip through the voids in the surface or the macrocycle cavities, guest molecule **8** used here is stoppered on one end through the xanthene unit, so that the accessibility of deeper macrocycle layers is significantly hampered.

In addition to UV/Vis spectroscopy, the surfaces have been analyzed with XPS (see the Supporting Information) and NEXAFS spectroscopy. As glass slides are not suitable for these methods, silicon surfaces have been used that have been prepared in the same way as the glass slides used before. Surfaces with three layers of macrocycle with and without incorporated *cis*-**8** have been prepared and analyzed. In addition, a thin film of **8** was deposited on a cleaned silicon surface via a drop-coating from CH_2Cl_2.

The N K-edge NEXAFS spectrum of the macrocycle multilayer in Figure 5a shows three clearly visible peaks that are assigned to the terpyridine moiety (398.7 and 399.3 eV) as well as to the amide nitrogens of the macrocycle (400.6 eV). In the spectrum of dropcoated **8** (Figure 5d), two resonances for the excitation into π* orbitals at 398.6 and 401.9 eV are found that can be assigned to the azobenzene- and diketopiperazine-nitrogen atoms. While these resonances are absent in the N K-edge NEXAFS spectra of the pristine macrocycle multilayers and those treated with *trans*-**8** (Figure 5b), they are present in the spectra of the multilayers treated with *cis*-**8** (Figure 5c), clearly showing the presence of *cis*-**8** on the surface and indicating the incorporation of the guest into the macrocycle multilayers (Figure 5). To get a more detailed insight to the packing of macrocycles with and without *cis*-**8**, angle-dependent C K-edge NEXAFS spectra have been recorded (Figure 6). The pristine macrocycle multilayer (Figure 6a) shows effects analogous to those observed in earlier studies of macrocycles on a terpyridine-terminated template with gold as the substrate.[30] The π* resonance exhibits splitting into two characteristic peaks at 285.1 and 285.4 eV, which show a clear linear dichroism in the 90–30° difference spectrum in line with the earlier results. This also includes a significant change of the relative heights of the two peaks.[31] When the multilayer is treated with *trans*-**8** solution (Figure 6b), the spectra closely resemble those of the pristine multilayer with comparable effects. In contrast, the surface treated with *cis*-**8** exhibits different spectra (Figure 6c). The signal at 285.4 eV seems to be superimposed by a second one and, furthermore, a signal at 288.3 eV shows up. When we look at the C–K edge of dropcoated **8** (Figure 6d), we can observe three characteristic signals at photon energies of 285.4, 287.2, and 288.3 eV, two of which can be assigned to the 'new' signals in the spectrum of the multilayer treated with a solution of *cis*-**8**. That we do not observe the third peak at 287.2 eV in this spectrum can be explained by its relatively low intensity and that it is therefore superimposed by the spectral contributions of the macrocycle multilayer. Together with the results from the N–K edge spectra, this is a clear evidence for the presence of the guest **8** on the surface. If we look at the 90–30° difference spectrum of this sample, an increase—when compared to the one of the original multilayer—of the linear dichroism in the area in which the π* resonances appear becomes apparent; this indicates the incorporation of the guest into the cavity of the macrocyles.

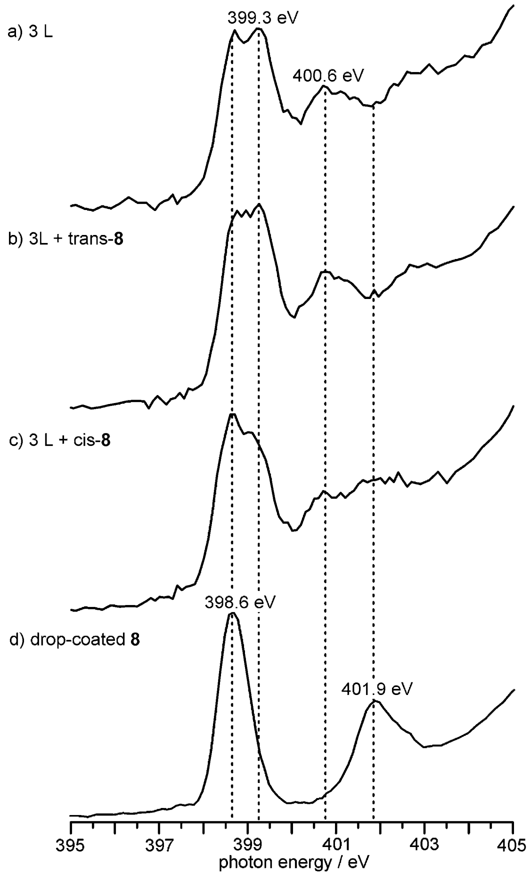

Figure 5. N K-edge NEXAFS spectra of a) a three-layered macrocycle multilayer, b) the multilayer treated with a solution of *trans*-**8** in the dark, c) the multilayer treated with a solution of *cis*-**8**, and d) the dropcoated **8**. Spectra were taken at an incidence angle of the linearly polarized synchrotron light of 55°.

To study on-surface switching, surfaces with one, three and five layers of macrocycles with bound *cis*-**8** have been irradiated first with light of $\lambda_2 = 470$ nm and then $\lambda_1 = 365$ nm over different times (1–30 min). None of these irradiations induced any changes in the absorption spectra of the surfaces, showing that the bound azobenzenes do not undergo *cis*-to-*trans* photoisomerization on the surface. Additionally, we tried to remove *cis*-**8** from the multilayer by washing the surfaces with different solvents. Immersing the surfaces in CH_2Cl_2 over 24 h had no effect on the surface, showing that **8** is quite strongly bound in the macrocycles. Next, the surfaces were irradiated in

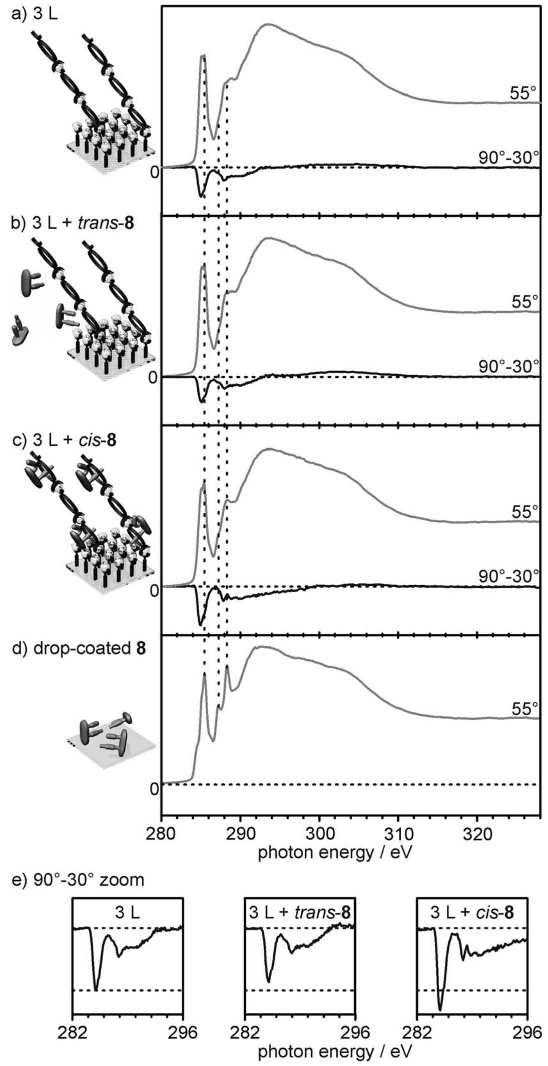

Figure 6. C K-edge NEXAFS spectra acquired at an incidence angle of the linearly polarized synchrotron light of (grey) 55° and (black) the difference between the spectra acquired at 90 and 30° of a) a three-layered macrocycle multilayer, b) the multilayer treated with a solution of *trans*-**8**, c) the multilayer treated with a solution of *cis*-**8**, and d) a cleaned surface drop-coated with a solution of **8**. e) Enhanced π^*-resonances in the 90–30° difference spectra displayed on identical scales.

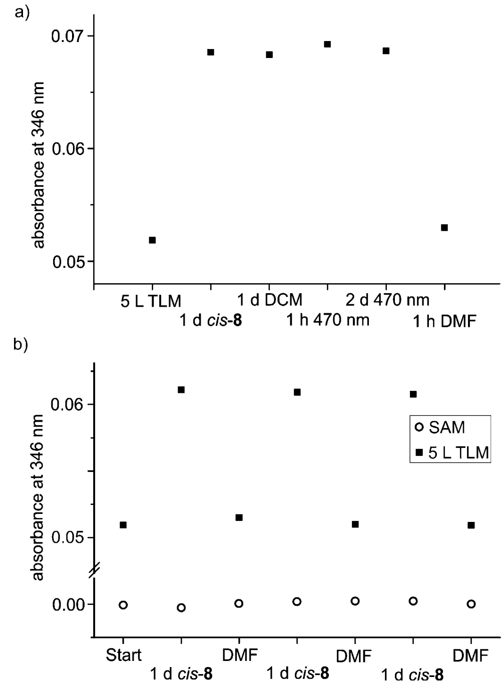

Figure 7. UV/Vis absorbance at 346 nm of surfaces: a) Removing **8** from five-layer surface. b) Reversibility of *cis*-**8** deposition on a five-layer surface versus no deposition on a SAM surface.

CH_2Cl_2 with visible light of $\lambda_2 = 470$ nm to find out if the back isomerization to *trans*-**8** is facilitated in a solution environment, but even after 48 h no change in the UV/Vis spectra was achieved. Guest *cis*-**8** could finally be removed from the multilayers by treating the surfaces with DMF, which acts as a competitive binder to the macrocycle. After 1 h in DMF, *cis*-**8** was completely removed from the multilayers, as followed by UV/Vis spectroscopy (Figure 7a). Reversibility was tested by alternating deposition and removal of **8** by 24 h immersion in a solution of **8** under UV irradiation and 1 h washing with DMF (Figure 7b). Although *cis*-to-*trans* isomerization of **8** occurs easily in solution by both equilibration in the dark or irradiation with visible light at $\lambda_2 = 470$ nm, it does not happen when *cis*-**8** is incorporated in macrocycle multilayers on a solid support. It appears that in the densely packed[30] multilayers, the freedom of *cis*-**8** to change its structure is too limited, thus blocking the *cis*-to-*trans* backswitching. This is in line with solid-state studies, showing the (photo-)isomerization of azobenzenes not to take place unless the molecules are specially designed to do so,[32] as the isomerization reaction requires a relatively large free volume[33] and is, therefore, hindered in densely packed structures.

Conclusion

A photoswitchable binding station for tetralactam macrocycles based on azobenzene as the photoswitchable element and diketopiperazine as the binding station has been developed. The *cis–trans* isomerization of the molecule and subsequent pseudorotaxane formation with a TLM was analyzed by UV/Vis and NMR spectroscopy. By using surfaces with multilayers of tetralactam macrocycles, a photocontrolled on-surface pseudorotaxane formation could be achieved, confirmed by UV/Vis, XPS, and NEXAFS spectroscopy. Additionally, NEXAFS spectra revealed an increase in the molecular order on the surface after pseudorotaxane formation. The ordered and densely packed nature of the multilayers on the surface prevents isomerization of the incorporated azobenzene guest molecules, illustrating the significant differences between solution and surface.

As pseudorotaxanes are precursors of mechanical interlocked molecules like rotaxanes, this work opens a path towards photoswitchable rotaxanes embedded in multilayers on surfaces leading in combination with chemically switchable rotaxanes to multi-stimuli responsive surface systems. The quite densely packed and oriented nature of the multilayers on the surface may result in concerted movement and potential macroscopic effects.

Acknowledgements

We are grateful to the Deutsche Forschungsgemeinschaft (SFB 765), the German Academic Exchange Service (DAAD) and the Academy of Finland (K.R.: Project Nos. 263256 and 292746). F.B.S. thanks the Beilstein Institut for a Ph.D. fellowship. The authors thank Dr. A. Nefedov (Karlsruhe Institute of Technology, KIT) from the HE-SGM Collaborate Research Group at the synchrotron facility BESSY II and Dr. O. Schwartzkopf, Dr. A. Vollmer, and M. Mast (all BESSY II) for support during our activities at HZB.

Keywords: azobenzene · photochemistry · pseudorotaxanes · supramolecular chemistry · surface chemistry

[1] a) E. R. Kay, D. A. Leigh, *Angew. Chem. Int. Ed.* **2015**, *54*, 10080 – 10088; *Angew. Chem.* **2015**, *127*, 10218 – 10226; b) M. Peplow, *Nature* **2015**, *525*, 18 – 21; c) S. Erbas-Cakmak, D. A. Leigh, C. T. McTernan, A. L. Nussbaumer, *Chem. Rev.* **2015**, *115*, 10081 – 10206.

[2] a) E. R. Kay, D. A. Leigh, F. Zerbetto, *Angew. Chem. Int. Ed.* **2007**, *46*, 72 – 191; *Angew. Chem.* **2007**, *119*, 72 – 196; b) J. Berná, D. A. Leigh, M. Lubomska, S. M. Mendoza, E. M. Perez, P. Rudolf, G. Teobaldi, F. Zerbetto, *Nat. Mater.* **2005**, *4*, 704 – 710; c) R. Eelkema, M. M. Pollard, J. Vicario, N. Katsonis, B. S. Ramon, C. W. M. Bastiaansen, D. J. Broer, B. L. Feringa, *Nature* **2006**, *440*, 163 – 163; d) Y. Liu, A. H. Flood, P. A. Bonvallet, S. A. Vignon, B. H. Northrop, H.-R. Tseng, J. O. Jeppesen, T. J. Huang, B. Brough, M. Baller, S. Magonov, S. D. Solares, W. A. Goddard, C.-M. Ho, J. F. Stoddart, *J. Am. Chem. Soc.* **2005**, *127*, 9745 – 9759; e) V. Balzani, A. Credi, M. Venturi, *ChemPhysChem* **2008**, *9*, 202 – 220.

[3] a) N. Katsonis, M. Lubomska, M. M. Pollard, B. L. Feringa, P. Rudolf, *Prog. Surf. Sci.* **2007**, *82*, 407 – 434; b) W. R. Browne, B. L. Feringa, *Annu. Rev. Phys. Chem.* **2009**, *60*, 407 – 428; c) M.-M. Russew, S. Hecht, *Adv. Mater.* **2010**, *22*, 3348 – 3360; d) R. Klajn in *Pure Appl. Chem., Vol. 82*, **2010**, p. 2247.

[4] a) J. C. Love, L. A. Estroff, J. K. Kriebel, R. G. Nuzzo, G. M. Whitesides, *Chem. Rev.* **2005**, *105*, 1103 – 1170; b) N. Herzer, S. Hoeppener, U. S. Schubert, *Chem. Commun.* **2010**, *46*, 5634 – 5652.

[5] S. Wang, Y. Song, L. Jiang, *J. Photochem. Photobiol. C* **2007**, *8*, 18 – 29.

[6] a) J. M. Mativetsky, G. Pace, M. Elbing, M. A. Rampi, M. Mayor, P. Samorì, *J. Am. Chem. Soc.* **2008**, *130*, 9192 – 9193; b) K. Smaali, S. Lenfant, S. Karpe, M. Oçafrain, P. Blanchard, D. Deresmes, S. Godey, A. Rochefort, J. Roncali, D. Vuillaume, *ACS Nano* **2010**, *4*, 2411 – 2421; c) M. del Valle, R. Gutierrez, C. Tejedor, G. Cuniberti, *Nat. Nano* **2007**, *2*, 176 – 179; d) N. Katsonis, T. Kudernac, M. Walko, S. J. van der Molen, B. J. van Wees, B. L. Feringa, *Adv. Mater.* **2006**, *18*, 1397 – 1400.

[7] a) F. L. Callari, S. Petralia, S. Conoci, S. Sortino, *New J. Chem.* **2008**, *32*, 1899 – 1903; b) Z. Wang, A.-M. Nygård, M. J. Cook, D. A. Russell, *Langmuir* **2004**, *20*, 5850 – 5857.

[8] R. A. van Delden, M. K. J. ter Wiel, M. M. Pollard, J. Vicario, N. Koumura, B. L. Feringa, *Nature* **2005**, *437*, 1337 – 1340.

[9] T. Hugel, N. B. Holland, A. Cattani, L. Moroder, M. Seitz, H. E. Gaub, *Science* **2002**, *296*, 1103 – 1106.

[10] a) C. A. Hunter, *J. Am. Chem. Soc.* **1992**, *114*, 5303 – 5311; b) F. Vögtle, S. Meier, R. Hoss, *Angew. Chem. Int. Ed. Engl.* **1992**, *31*, 1619 – 1622.

[11] R. Jäger, F. Vögtle, *Angew. Chem.* **1997**, *109*, 966 – 980.

[12] a) J. J. Richardson, M. Björnmalm, F. Caruso, *Science* **2015**, *348*, aaa2491; b) C. R. South, M. Weck, *Langmuir* **2008**, *24*, 7506 – 7511; c) V. Piñón, M. Weck, *Langmuir* **2012**, *28*, 3279 – 3284; d) M. Wanunu, R. Popovitz-Biro, H. Cohen, A. Vaskevich, I. Rubinstein, *J. Am. Chem. Soc.* **2005**, *127*, 9207 – 9215; e) Y. Chaikin, H. Leader, R. Popovitz-Biro, A. Vaskevich, I. Rubinstein, *Langmuir* **2011**, *27*, 1298 – 1307; f) P. C. Mondal, J. Yekkoni Lakshmanan, H. Hamoudi, M. Zharnikov, T. Gupta, *J. Phys. Chem. C* **2011**, *115*, 16398 – 16404; g) T. Gupta, P. C. Mondal, A. Kumar, Y. L. Jeyachandran, M. Zharnikov, *Adv. Funct. Mater.* **2013**, *23*, 4227 – 4235.

[13] a) G. de Ruiter, M. Lahav, M. E. van der Boom, *Acc. Chem. Res.* **2014**, *47*, 3407 – 3416; b) M. Altman, A. D. Shukla, T. Zubkov, G. Evmenenko, P. Dutta, M. E. van der Boom, *J. Am. Chem. Soc.* **2006**, *128*, 7374 – 7382; c) N. Tuccitto, I. Delfanti, V. Torrisi, F. Scandola, C. Chiorboli, V. Stepanenko, F. Wurthner, A. Licciardello, *Phys. Chem. Chem. Phys.* **2009**, *11*, 4033 – 4038; d) N. Tuccitto, V. Ferri, M. Cavazzini, S. Quici, G. Zhavnerko, A. Licciardello, M. A. Rampi, *Nat. Mater.* **2009**, *8*, 41 – 46.

[14] T. Heinrich, C. H. H. Traulsen, M. Holzweber, S. Richter, V. Kunz, S. K. Kastner, S. O. Krabbenborg, J. Huskens, W. E. S. Unger, C. A. Schalley, *J. Am. Chem. Soc.* **2015**, *137*, 4382 – 4390.

[15] H. M. D. Bandara, S. C. Burdette, *Chem. Soc. Rev.* **2012**, *41*, 1809 – 1825.

[16] a) M. Baroncini, S. Silvi, M. Venturi, A. Credi, *Angew. Chem. Int. Ed.* **2012**, *51*, 4223 – 4226; *Angew. Chem.* **2012**, *124*, 4299 – 4302; b) T. Avellini, H. Li, A. Coskun, G. Barin, A. Trabolsi, A. N. Basuray, S. K. Dey, A. Credi, S. Silvi, J. F. Stoddart, M. Venturi, *Angew. Chem. Int. Ed.* **2012**, *51*, 1611 – 1615; *Angew. Chem.* **2012**, *124*, 1643 – 1647.

[17] R. Klajn, J. F. Stoddart, B. A. Grzybowski, *Chem. Soc. Rev.* **2010**, *39*, 2203 – 2237.

[18] a) A. C. Fahrenbach, S. C. Warren, J. T. Incorvati, A.-J. Avestro, J. C. Barnes, J. F. Stoddart, B. A. Grzybowski, *Adv. Mater.* **2013**, *25*, 331 – 348; b) R. H. El Halabieh, O. Mermut, C. J. Barrett in *Pure Appl. Chem. Vol. 76*, **2004**, p. 1445; c) H. S. Lim, J. T. Han, D. Kwak, M. Jin, K. Cho, *J. Am. Chem. Soc.* **2006**, *128*, 14458 – 14459.

[19] a) I. Willner, V. Pardo-Yissar, E. Katz, K. T. Ranjit, *J. Electroanal. Chem.* **2001**, *497*, 172 – 177; b) D. Patra, H. Zhang, S. Sengupta, A. Sen, *ACS Nano* **2013**, *7*, 7674 – 7679; c) P. Wan, Y. Jiang, Y. Wang, Z. Wang, X. Zhang, *Chem. Commun.* **2008**, 5710 – 5712.

[20] D. Tarn, D. P. Ferris, J. C. Barnes, M. W. Ambrogio, J. F. Stoddart, J. I. Zink, *Nanoscale* **2014**, *6*, 3335 – 3343.

[21] a) K.-S. Jeong, K.-J. Chang, Y.-J. An, *Chem. Commun.* **2003**, 1450 – 1451; b) K.-J. Chang, Y.-J. An, H. Uh, K.-S. Jeong, *J. Org. Chem.* **2004**, *69*, 6556 – 6563.

[22] H. Adams, F. J. Carver, C. A. Hunter, N. J. Osborne, *Chem. Commun.* **1996**, 2529 – 2530.

[23] S. A. Nagamani, Y. Norikane, N. Tamaoki, *J. Org. Chem.* **2005**, *70*, 9304 – 9313.

[24] a) K. C. Majumdar, K. Ray, S. Ganai, *Synlett* **2010**, 2122 – 2124; b) R. M. Williams, J. Cao, H. Tsujishima, R. J. Cox, *J. Am. Chem. Soc.* **2003**, *125*, 12172 – 12178.

[25] B. Baytekin, S. S. Zhu, B. Brusilowskij, J. Illigen, J. Ranta, J. Huuskonen, L. Russo, K. Rissanen, L. Kaufmann, C. A. Schalley, *Chem. Eur. J.* **2008**, *14*, 10012 – 10028.

[26] R. J. Lindquist, K. M. Lefler, K. E. Brown, S. M. Dyar, E. A. Margulies, R. M. Young, M. R. Wasielewski, *J. Am. Chem. Soc.* **2014**, *136*, 14912 – 14923.

[27] J. Harada, K. Ogawa, S. Tomoda, *Acta Crystallogr. Sect. B* **1997**, *53*, 662 – 672.

[28] J. Griffiths, *Chem. Soc. Rev.* **1972**, *1*, 481 – 493.

[29] a) C. H. H. Traulsen, V. Kunz, T. Heinrich, S. Richter, M. Holzweber, A. Schulz, L. K. S. von Krbek, U. T. J. Scheuschner, J. Poppenberg, W. E. S. Unger, C. A. Schalley, *Langmuir* **2013**, *29*, 14284-14292; b) S. Richter, C. H. H. Traulsen, T. Heinrich, J. Poppenberg, C. Leppich, M. Holzweber, W. E. S. Unger, C. A. Schalley, *J. Phys. Chem. C* **2013**, *117*, 18980 – 18985; c) S. Richter, J. Poppenberg, C. H. H. Traulsen, E. Darlatt, A. Sokolowski, D. Sattler, W. E. S. Unger, C. A. Schalley, *J. Am. Chem. Soc.* **2012**, *134*, 16289 – 16297.

[30] J. Poppenberg, S. Richter, C. H. H. Traulsen, E. Darlatt, B. Baytekin, T. Heinrich, P. M. Deutinger, K. Huth, W. E. S. Unger, C. A. Schalley, *Chem. Sci.* **2013**, *4*, 3131 – 3139.

[31] One might say that the effect is rather small for a multilayer of molecules that large and therefore the molecules are not well-ordered. However, as we already stated earlier,[11,27] the different orientations of the aromatic rings in the molecules prevent larger effects.

[32] a) M. Baroncini, S. d'Agostino, G. Bergamini, P. Ceroni, A. Comotti, P. Sozzani, I. Bassanetti, F. Grepioni, T. M. Hernandez, S. Silvi, M. Venturi, A. Credi, *Nat. Chem.* **2015**, *7*, 634 – 640; b) O. S. Bushuyev, A. Tomberg, T. Friščić, C. J. Barrett, *J. Am. Chem. Soc.* **2013**, *135*, 12556 – 12559; c) H. Koshima, N. Ojima, H. Uchimoto, *J. Am. Chem. Soc.* **2009**, *131*, 6890 – 6891.

[33] J. G. Victor, J. M. Torkelson, *Macromolecules* **1987**, *20*, 2241 – 2250.

Received: July 1, 2016